Geol. Mag. **153** (*1*), *2016, pp. 179–192.* © *Cambridge University Press 2015*
doi:10.1017/S0016756815000692

RAPID COMMUNICATION

Crustal geodynamics from the Archaean Bundelkhand Craton, India: constraints from zircon U–Pb–Hf isotope studies

L. SAHA*‡†, D. FREI§, A. GERDES¶, J. K. PATI||, S. SARKAR*, V. PATOLE#, A. BHANDARI* & P. NASIPURI#

*Department of Earth Sciences, Indian Institute of Technology, Roorkee, India
‡School of Agricultural, Earth and Environmental Sciences, University of KwaZulu-Natal, Durban, South Africa
§Central Analytical Facility, Stellenbosch University, South Africa
¶Institute of Geosciences, Goethe University Frankfurt, Altenhöferallee 1, 60438 Frankfurt am Main, Germany
||Department of Earth and Planetary Sciences, University of Allahabad, India
#Department of Earth and Environmental Sciences, Indian Institute of Science Education and Research-Bhopal, India

(*Received* 23 March 2015; *accepted* 18 August 2015; *first published online* 21 October 2015)

Abstract

A comprehensive study based on U–Pb and Hf isotope analyses of zircons from gneisses has been conducted along the western part (Babina area) of the E–W-trending Bundelkhand Tectonic Zone in the central part of the Archaean Bundelkhand Craton. ^{207}Pb–^{206}Pb zircon ages and Hf isotopic data indicate the existence of a felsic crust at ~ 3.59 Ga, followed by a second tectonothermal event at ~ 3.44 Ga, leading to calc-alkaline magmatism and subsequent crustal growth. The study hence suggests that crust formation in the Bundelkhand Craton occurred in a similar time-frame to that recorded from the Singhbhum and Bastar cratons of the North Indian Shield.

Keywords: Bundelkhand Craton, Bundelkhand Tectonic Zone, Archaean, tonalite–trondhjemite–granodiorite gneiss (TTG), U–Pb zircon ages.

1. Introduction

Tonalite–trondhjemite–granodiorite (TTG) rocks are the major components of Archaean continental crust (Condie, 2000). Available evidence from zircon geochemistry and U–Pb geochronology suggests that continental crust has been forming since ~ 4.4 Ga (Wilde *et al.* 2001). Although the existence of 4.4 Ga old crust (Wilde *et al.* 2001) is disputable, magmatic emplacement ages of TTG rocks clustering around ~ 3.9–3.8 Ga are reported from the Itsaq Gneiss Complex and Saglek–Hebron Block in the North Atlantic Craton, the Napier Complex in Antarctica and the North China Craton, and such rocks also yielded abundant detrital grains to the Jack Hills Quartzite in Western Australia (Myers, 1988; Nutman *et al.* 1992; Friend & Nutman, 2005). These occurrences indicate widespread continental crust formation from ~ 3.8 Ga onwards (for detailed discussions see van Kranendonk, Smithies & Bennett, 2007). In peninsular India, relatively younger crust formation ages have been reported for trondhjemite and leucogranite from the Bastar Craton (3.5–3.4 Ga; Sarkar *et al.* 1993; Ghosh, 2004), felsic volcanic and trondhjemitic xenoliths from the Singhbhum Craton (~ 3.4 Ga; Sengupta *et al.* 1996; Mishra *et al.* 1999) and TTG from the Bundelkhand Craton (~ 3.6 Ga; Kaur, Zeh & Chaudhri, 2014). Apart from sparse zircon ages recorded from a few localities in these cratons, no comprehensive study has been conducted to chart the processes related to the origin of Archaean continental crust in these Indian cratons.

Geochronological studies based on combined U–Pb and Lu–Hf systematics of zircon are considered to be very powerful tools to understand the timing and processes of formation of Archaean crust, their recycling and related magma generation processes (Condie, 2000; Kröner *et al.* 2014). The U, Pb and Hf contents in magmatic zircons are usually high and the mineral can even preserve original isotopic compositions under extreme granulite facies conditions. Consequently, they can be used as a geochronometer to constrain crustal formation and subsequent recycling processes (Nutman *et al.* 2007, 2000; Iizuka *et al.* 2007; Harrison *et al.* 2008; Nebel-Jacobsen *et al.* 2010).

In this study we present new U–Pb zircon ages and Lu–Hf isotope data from the TTG gneisses of the Bundelkhand Craton, North Central India, in order to constrain the timing of Palaeoarchaean crustal building processes (Fig. 1).

2. Geological background

The Bundelkhand Craton forms the eastern part of the Aravalli–Bundelkhand protocontinent (Mondal *et al.* 2002). Proterozoic sedimentary basins (Vindhyan Basin) and tectonic belts (Central Indian Tectonic Zone) separate the Bundelkhand Craton from the Aravalli Craton to the west, the Singhbhum Craton to the east and the Bastar Craton to the south (Fig. 1a). The northern part of the Bundelkhand Craton is mostly covered by Indo-Gangetic alluvium. Major lithological components of the craton are intensely deformed granitoid-greenstone terrains that are intruded by undeformed granitoids (Basu, 1986; Sharma & Rahman, 2000; Pati *et al.* 2007; Meert *et al.* 2010; Fig. 1b).

The oldest crustal components of the craton are represented by the ~ 3.58–3.5 Ga trondhjemitic gneisses from Baghora (whole-rock Rb–Sr age) and Mauranipur (U–Pb zircon ages) in the central part of the craton (Sarkar, Paul & Potts, 1996; Kaur, Zeh & Chaudhri, 2014). Mondal *et al.*

†Author for correspondence: saha.lopamudra@gmail.com

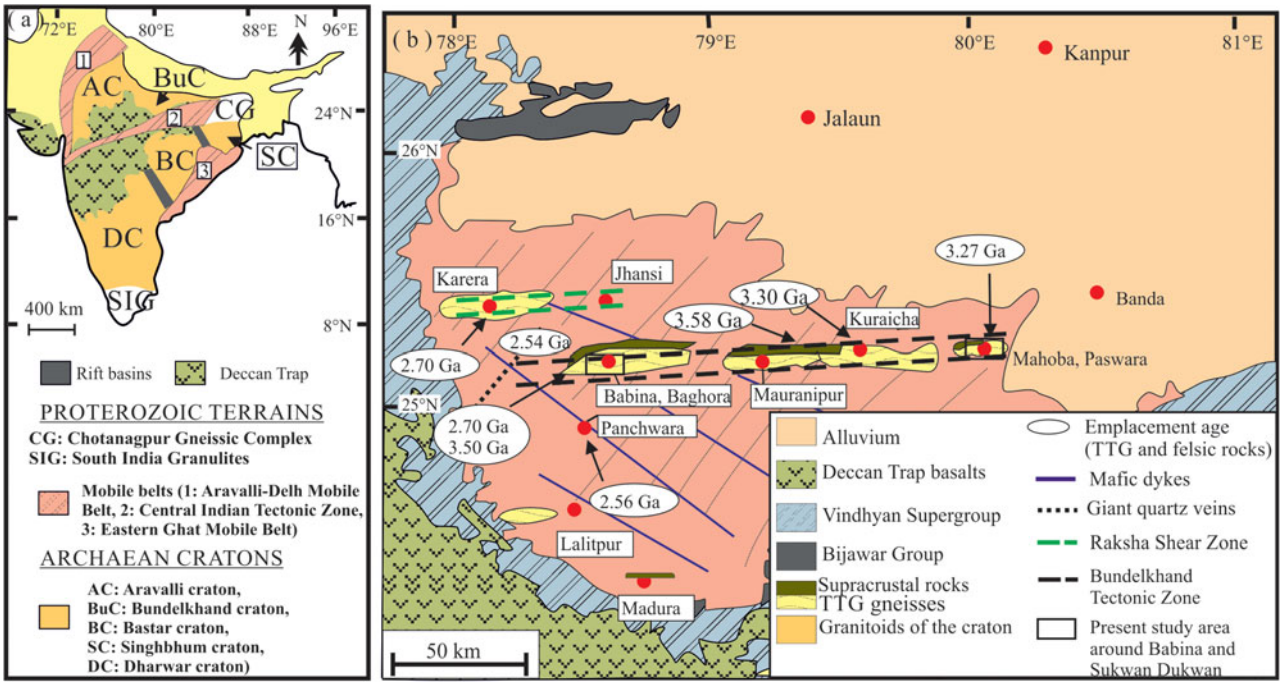

Figure 1. (Colour online) (a) Tectonic map of peninsular India showing the location of the Bundelkhand Craton with respect to the Archaean cratons and Proterozoic mobile belts. (b) Geological map of the Bundelkhand Craton modified after Basu (1986) showing the geochronological data from different terrains (after Mondal *et al*. 2002; Kaur, Zeh & Chaudhri, 2014) and localities of the present study (represented by the box).

(2002) reported zircon evaporation ages of ~ 3.3–3.2 Ga for high-aluminium trondhjemite gneiss from Kuraicha and Mahoba and tonalitic gneisses from Panchwara. Neoarchaean zircon evaporation ages and SHRIMP ages of ~ 2.7 and 2.5 Ga, have been recorded for tonalite gneiss, granitoids and felsic schists from the central Bundelkhand Craton (Fig. 1b; Mondal *et al.* 2002; Kumar *et al.* 2011; Singh & Slabunov, 2014). Geochemical signatures of the craton's Mesoarchaean TTG gneisses indicate emplacement in a suprasubduction environment (Ram Mohan *et al.* 2012).

Nd isotopic data for the amphibolites in the Mahoba, Mauranipur and Babina areas indicate depleted mantle model ages of ~ 3.4–3.3 Ga, suggesting an origin of these mafic supracrustal rocks from a depleted mantle during the Mesoarchaean Era (Malviya, Arima & Pati, 2005). An intrusive contact of the ~ 3.3 Ga old Mahoba TTG gneiss with the associated supracrustal units and a zircon evaporation age of ~ 3.25 Ga obtained from a metabasic enclave within the gneiss indicate the minimum age of formation of the supracrustal units (Mondal *et al.* 2002). The last phase of magmatism in the craton was the intrusion of the NW-trending mafic dykes between ~ 1.97 and 1.8 Ga (Pradhan *et al.* 2012).

Lead-loss events and post-magmatic overgrowth on magmatic zircons from the TTG gneisses around the Mahoba and Lalitpur areas occurred at ~ 3.1 Ga, ~ 3.05 Ga and ~ 2.9–2.8 Ga, and have been interpreted by Mondal *et al.* (2002) as ages of metamorphism. The sole well-constrained study on the metamorphism of the craton was conducted by Saha *et al.* (2011) on the corundum-bearing white-schist in the Babina area (occurring in the western part of the Bundelkhand Tectonic Zone), where the authors noted a ~ 2.78 Ga high-pressure metamorphic event indicating the occurrence of collisional tectonics. Geochemical signatures (strong heavy rare earth element depletion) of Neoarchaean felsic rocks in the craton indicate their emplacement in a convergence setting (Mondal *et al.* 2002; Kumar *et al.* 2011; Singh & Slubanov, 2014). Thus, collisional tectonics played a major role in the stabilization of the craton in the Neoarchaean Era.

3. Field observations

Near Babina, scattered outcrops of TTG gneisses show development of alternating leucocratic and melanocratic bands with mafic (amphibolite) enclaves displaying local partial melting (Fig. 2). The extremely deformed outcrops (Fig. 2c) indicate that the TTG gneisses have experienced multiple episodes of folding. Two samples of TTG gneisses, LB13 and DUR13, were collected from the Babina area for this study (Fig. 1b).

4. Zircon geochronology

4.a. U–Pb method

Zircon U–Pb age data were acquired at the Central Analytical Facility, Stellenbosch University, by laser ablation single-collector magnetic sector field inductively coupled plasma mass spectrometry (LA-SF-ICP-MS) employing a Thermo Finnigan Element 2 mass spectrometer coupled to a NewWave UP213 laser ablation system. All age data were obtained by single spot analyses with a spot diameter of 30 µm and a crater depth of approximately 15–20 µm (online Supplementary Material available from http://journals.cambridge.org/geo). The methods employed for analysis and data processing are described in detail by Gerdes & Zeh (2006, 2009) and Frei & Gerdes (2009). For quality control, the Plešovice (Sláma *et al.* 2008) and M127 (Nasdala *et al.* 2008; Mattinson, 2010) zircon reference materials were analysed, and the results were consistently in excellent agreement with the published ID-TIMS ages. Full analytical details and the results for all

https://doi.org/10.1017/S0016756815000692 Published online by Cambridge University Press

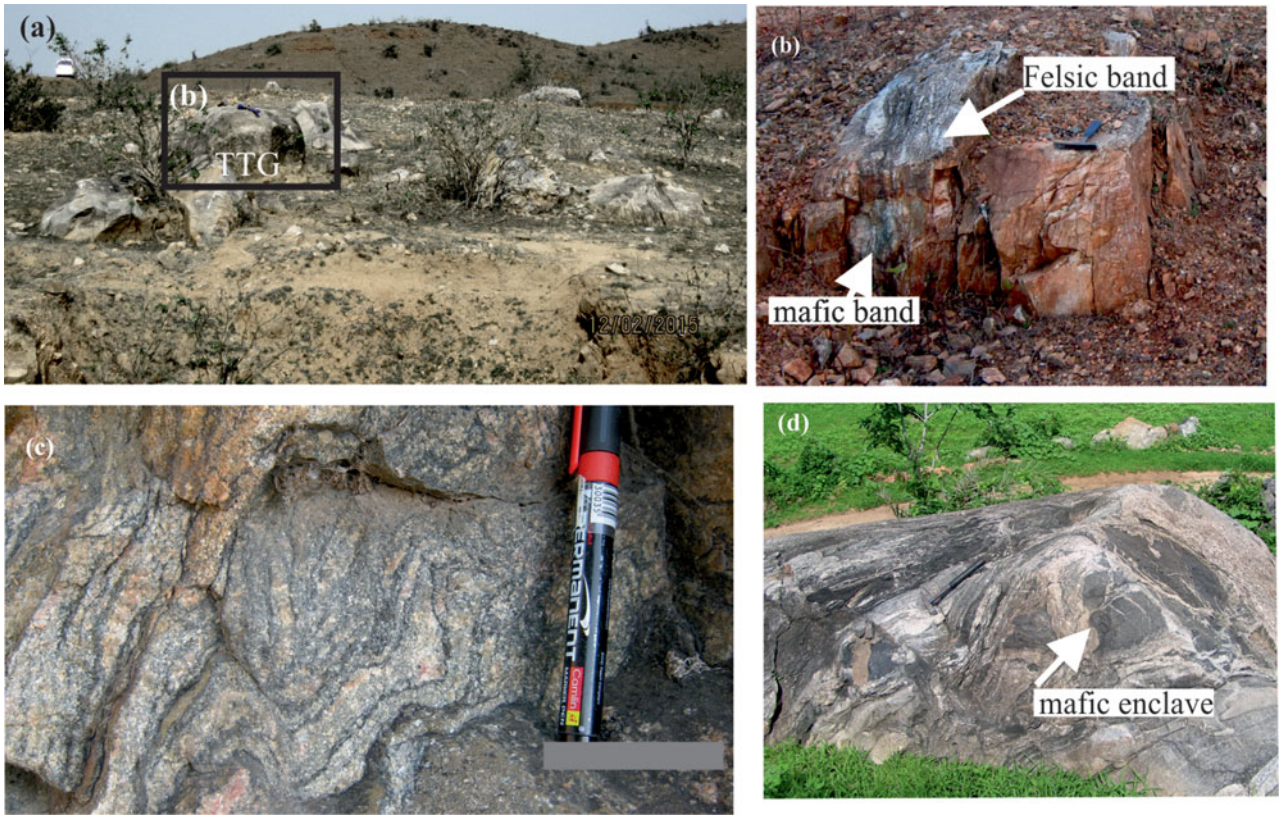

Figure 2. (Colour online) Field photographs of the TTGs from the Babina and Sukwan–Dukwan dam areas. (a) TTG gneiss from the Babina area (sample LB13); (b) banding and foliation in the TTG gneiss; length of hammer for scale is 40 cm; (c) migmatitic banding in the TTG gneiss; length of pen for scale is 14 cm; (d) large-size mafic enclaves in the TTG gneiss; length of hammer for scale is 29 cm.

quality control materials analysed are reported in Table S1 in the online Supplementary Material (available at http://journals.cambridge.org/geo). The calculation of concordia ages and plotting of concordia diagrams were performed using Isoplot/Ex 3.0 (Ludwig, 2003).

4.b. Zircon data from the TTG gneiss near Babina (LB13)

Cathodoluminescence (CL) imaging reveals that most zircons separated from LB13 show oscillatory magmatic zoning (Fig. 3a, b). Some zircons show cores that are apparently overgrown by rims displaying oscillatory zoning; however, no age differences could be found between cores and rims, suggesting that individual zircon grains have been formed during a single magmatic event. In total 40 single spot analyses on 29 grains have been obtained. Although secondary textural features (e.g. alteration, metamictization and recrystallization) are not widespread as observed in CL images, a significant portion of the analyses yielded discordant ages (60 % of the analyses are > 10 % discordant; Table 1; Fig. 3c). In general, all analyses that yielded highly discordant ages also have U contents > 500 ppm, pointing to metamictization which enhanced lead loss. Subsequent Lu–Hf analyses (discussed in Section 5) have only been performed on those spots that yielded > 90 % U–Pb concordance. As shown in a Wetherill Concordia plot in Figure 3c, the concordant to near-concordant analyses define two distinct age groups: *c*. 3.59 Ga and *c*. 3.44 Ga. The older zircon grains give an upper intercept age of 3589 ± 7 Ma (MSWD = 0.83), identical to a concordia age of 3589 ± 8 Ma (MSWD = 0.21) for the eight most concordant analyses. The younger zircon age group gives an upper intercept age of 3444 ± 26 Ma (MSWD = 2.7) and a mean Pb–Pb age of 3440 ± 3 Ma (MSWD = 0.83) for the four most concordant analysis. The data suggest that the younger ages reflect the timing of intrusion of TTG magmatism. The older zircon grains possibly represent xenocrysts derived from an older crustal component.

4.c. Zircon data from the TTGs of the Sukwan–Dukwan dam area (DUR13)

The CL images of the zircons separated from DUR13 (Fig. 4a, b) show that all zircons are affected by a strong metamictization that in many cases has led to a dominant secondary alteration and recrystallization of the grains. A sufficient number of grains still exhibit magmatic oscillatory zoning, predominantly in the tips of individual zircon crystals, and these areas have been the primary targets for U–Pb age analysis. However, with the exception of one analysis that yielded a near-concordant Pb–Pb age of 3368 ± 30 Ma (94 % concordant, analysis 46 in Table 2 and Fig. 4b) and a comparatively low U content of 79 ppm, all analysis yielded ages that are highly discordant (74 to 26 % discordance, Table 2), indicating large degrees of lead loss. The observed large extent of lead loss is in accordance with the very high U contents that range from 264 to 3274 ppm and are above 800 ppm for > 90 % of the analyses. Consequently, the calculated discordia yields poorly defined upper (3220 ± 79 Ma)

https://doi.org/10.1017/S0016756815000692 Published online by Cambridge University Press

Table 1. U–Pb data for the zircons from the TTG gneiss of the Babina area (LB13)

Analysis	U [a] (ppm)	Pb[a] (ppm)	Th/U[a]	$^{207}Pb/^{235}U$[b]	2 σ[d]	$^{206}Pb/^{238}U$[b]	2 σ[d]	rho[c]	$^{207}Pb/^{206}Pb$[e]	2 σ[d]	$^{207}Pb/^{235}U$	2 σ	$^{206}Pb/^{238}U$	2 σ	$^{207}Pb/^{206}Pb$ (Ma)	2 σ	%
zircon 07	613	225	1.05	8.32	0.28	0.265	0.008	0.93	0.228	0.003	2267	77	1516	48	3035	10	50
zircon 08	813	307	0.51	9.46	0.43	0.297	0.013	0.95	0.231	0.003	2383	108	1675	72	3061	12	55
zircon 09	1588	249	0.15	2.63	0.16	0.132	0.007	0.87	0.144	0.004	1308	82	802	44	2273	27	35
zircon 10	404	358	0.53	31.79	1.00	0.713	0.021	0.96	0.323	0.003	3544	111	3471	104	3585	7	97
zircon 11	522	214	0.94	10.89	0.34	0.303	0.009	0.96	0.261	0.002	2514	77	1706	50	3251	7	52
zircon 13	470	277	0.44	19.80	0.66	0.479	0.016	0.97	0.300	0.002	3082	103	2521	82	3471	6	73
zircon 14	628	249	0.28	9.62	0.33	0.356	0.012	0.94	0.196	0.002	2399	83	1963	64	2792	10	70
zircon 16	620	151	0.08	5.21	0.37	0.207	0.014	0.94	0.183	0.004	1855	132	1213	81	2678	20	45
zircon 20	234	194	0.29	31.20	1.02	0.692	0.021	0.93	0.327	0.004	3525	115	3392	103	3602	9	94
zircon 21	139	129	0.54	33.26	1.07	0.742	0.023	0.96	0.325	0.003	3588	116	3580	112	3593	7	100
zircon 22	998	316	0.68	7.68	0.30	0.261	0.009	0.89	0.214	0.004	2194	85	1494	52	2932	14	51
zircon 23	747	233	0.55	5.75	0.28	0.198	0.008	0.85	0.211	0.005	1939	93	1164	48	2912	20	40
zircon 24	520	222	1.13	10.22	0.49	0.315	0.014	0.93	0.235	0.004	2455	117	1765	78	3089	14	57
zircon 25	165	163	1.52	28.59	1.08	0.644	0.022	0.90	0.322	0.005	3439	130	3203	108	3580	13	89
zircon 26	353	244	0.82	20.93	0.69	0.538	0.017	0.94	0.282	0.003	3135	103	2777	86	3374	9	82
zircon 27	114	91	0.72	24.83	0.91	0.636	0.021	0.92	0.283	0.004	3302	120	3174	107	3380	11	94
zircon 28	663	223	0.14	9.76	0.82	0.289	0.023	0.93	0.245	0.007	2412	204	1636	129	3153	24	52
zircon 29	308	256	0.10	31.58	1.12	0.710	0.024	0.97	0.323	0.003	3537	126	3458	119	3582	7	97
zircon 33	185	147	0.25	29.66	1.02	0.667	0.022	0.96	0.323	0.003	3476	120	3293	109	3583	7	95
zircon 34	329	243	0.21	25.19	1.02	0.632	0.023	0.89	0.289	0.005	3315	134	3159	114	3411	14	93
zircon 35	156	144	1.06	28.42	0.95	0.699	0.023	0.97	0.295	0.002	3434	114	3417	111	3443	6	99
zircon 36	231	148	0.27	21.22	0.78	0.522	0.018	0.93	0.295	0.004	3149	116	2706	93	3444	11	79
zircon 37	155	138	0.97	27.91	0.87	0.689	0.020	0.95	0.294	0.003	3416	106	3378	100	3438	8	98
zircon 46	233	204	0.12	33.44	1.27	0.748	0.027	0.97	0.324	0.003	3594	136	3600	132	3590	8	100
zircon 47	279	173	0.27	18.68	0.65	0.534	0.017	0.94	0.254	0.003	3026	105	2758	90	3208	9	86
zircon 48	336	332	1.00	33.28	1.26	0.748	0.028	0.97	0.323	0.003	3589	136	3600	133	3583	7	100
zircon 49	225	192	0.41	29.18	0.84	0.705	0.020	0.97	0.300	0.002	3460	100	3440	96	3471	6	99
zircon 50	466	351	0.19	27.37	1.48	0.629	0.034	0.99	0.316	0.002	3397	183	3145	168	3549	5	89
zircon 51	773	308	0.05	12.05	0.46	0.335	0.012	0.92	0.261	0.004	2609	99	1864	65	3251	12	57
zircon 52	254	213	1.28	21.40	0.79	0.561	0.020	0.96	0.277	0.003	3157	117	2869	103	3345	8	86
zircon 53	207	155	0.46	24.58	0.74	0.614	0.018	0.97	0.290	0.002	3292	98	3087	89	3419	6	90
zircon 55	549	242	0.82	11.62	0.56	0.338	0.016	0.97	0.249	0.003	2574	123	1877	87	3180	9	59
zircon 59	377	290	0.44	24.50	0.75	0.598	0.017	0.95	0.297	0.003	3289	100	3020	87	3456	7	87
zircon 60	147	123	0.55	27.41	0.85	0.675	0.020	0.96	0.294	0.003	3398	105	3326	99	3441	7	97
zircon 61	136	130	1.10	28.69	1.00	0.708	0.024	0.96	0.294	0.003	3443	121	3452	116	3438	7	100
zircon 62	211	160	1.00	21.13	0.76	0.513	0.017	0.93	0.298	0.004	3145	113	2671	90	3462	10	77
zircon 63	678	318	0.93	10.20	0.82	0.302	0.024	0.98	0.245	0.004	2454	198	1701	134	3154	13	54
zircon 65	135	122	0.36	33.37	1.08	0.745	0.021	0.87	0.325	0.005	3591	116	3588	101	3593	12	100
zircon 67	1106	398	0.31	6.77	0.32	0.287	0.010	0.70	0.171	0.006	2082	99	1626	55	2569	28	63
zircon 68	381	208	0.71	15.36	0.92	0.454	0.026	0.94	0.245	0.005	2838	170	2413	136	3155	16	76

[a]U and Pb concentrations and Th/U ratios are calculated relative to the GJ-1 reference zircon
[b]Corrected for background and within-run Pb/U fractionation and normalized to reference zircon GJ-1 (ID-TIMS values/measured value); $^{207}Pb/^{235}U$ calculated using ($^{207}Pb/^{206}Pb$)/($^{238}U/^{206}Pb$ * 1/137.88)
[c]Rho is the error correlation defined as the quotient of the propagated errors of the $^{206}Pb/^{238}U$ and the $^{207}Pb/^{235}U$ ratios
[d]Quadratic addition of within-run errors (2 s.d.) and daily reproducibility of GJ-1 (2 s.d)
[e]Corrected for mass-bias by normalizing to the GJ-1 reference zircon (~ 0.6 per atomic mass unit) and common Pb using the model Pb composition of Stacey &Kramers (1975)

Table 2. U–Pb data for zircons from the TTG gneiss of the Sukwan–Dukwan area (DUR13)

Analysis	U [a] (ppm)	Pb [a] (ppm)	Th/U[a]	$^{207}Pb/^{235}U$[b]	2 σ[d]	$^{206}Pb/^{238}U$[b]	2 σ[d]	rho[c]	$^{207}Pb/^{206}Pb$[e]	2 σ[d]	$^{207}Pb/^{235}U$	2 σ	$^{206}Pb/^{238}U$	2 σ	$^{207}Pb/^{206}Pb$ (Ma)	2 σ	%
Zircon 07	1316	275	0.08	6.76	0.27	0.209	0.008	0.94	0.2345	0.0066	2081	83	1225	41	3083	22	40
Zircon 08	790	123	0.03	3.24	0.13	0.156	0.006	0.92	0.1511	0.0049	1467	60	933	33	2358	27	40
Zircon 10	1497	179	0.03	1.80	0.07	0.119	0.004	0.92	0.1090	0.0035	1044	42	728	26	1783	29	41
Zircon 11	3274	255	0.02	0.93	0.04	0.078	0.003	0.91	0.0870	0.0029	670	27	483	17	1361	32	36
Zircon 12	1345	161	0.07	2.48	0.10	0.120	0.005	0.92	0.1502	0.0049	1267	52	730	26	2348	28	31
Zircon 13	921	165	0.18	5.45	0.22	0.179	0.007	0.93	0.2212	0.0066	1893	76	1060	37	2989	24	35
Zircon 14	1328	169	0.27	2.30	0.09	0.127	0.005	0.92	0.1312	0.0041	1213	49	772	27	2114	27	37
Zircon 15	833	285	0.20	9.01	0.36	0.342	0.013	0.93	0.1908	0.0056	2339	93	1898	61	2749	24	69
Zircon 16	289	99	0.68	10.92	0.45	0.342	0.013	0.92	0.2314	0.0073	2516	103	1897	62	3062	25	62
Zircon 20	1618	196	0.05	2.05	0.08	0.121	0.005	0.92	0.1225	0.0039	1133	46	739	26	1993	28	37
Zircon 22	1611	307	0.39	6.18	0.25	0.190	0.007	0.92	0.2357	0.0076	2002	82	1123	39	3091	25	36
Zircon 23	1164	192	0.02	3.66	0.15	0.165	0.006	0.92	0.1613	0.0053	1563	64	983	34	2469	27	40
Zircon 24	1370	180	0.02	2.59	0.11	0.132	0.005	0.91	0.1431	0.0047	1299	53	797	28	2265	28	35
Zircon 25	1485	144	0.21	1.38	0.06	0.097	0.004	0.91	0.1029	0.0036	879	36	597	21	1677	32	36
Zircon 26	718	126	0.63	4.11	0.17	0.175	0.007	0.91	0.1698	0.0059	1656	69	1042	36	2556	29	41
Zircon 27	651	220	0.09	9.68	0.41	0.337	0.013	0.91	0.2084	0.0074	2405	101	1872	62	2893	29	65
Zircon 28	981	231	0.02	5.69	0.24	0.235	0.009	0.91	0.1756	0.0061	1930	80	1361	46	2612	29	52
Zircon 29	264	79	0.35	9.70	0.42	0.298	0.012	0.90	0.2360	0.0091	2407	104	1682	57	3094	30	54
Zircon 33	2925	279	0.03	1.77	0.08	0.095	0.004	0.89	0.1346	0.0051	1034	44	587	21	2159	33	27
Zircon 34	563	163	0.71	8.64	0.36	0.290	0.011	0.90	0.2163	0.0080	2301	97	1640	55	2953	29	56
Zircon 35	2724	257	0.06	1.37	0.06	0.094	0.004	0.89	0.1055	0.0042	876	38	580	21	1723	36	34
Zircon 36	978	166	0.18	4.15	0.18	0.170	0.006	0.89	0.1770	0.0069	1663	71	1012	36	2625	32	39
Zircon 37	1349	141	0.03	1.49	0.06	0.104	0.004	0.88	0.1039	0.0042	928	40	639	23	1694	36	38
Zircon 46	79	50	0.41	24.59	1.39	0.635	0.034	0.94	0.2808	0.0108	3292	186	3170	133	3368	30	94
Zircon 47	1051	268	0.32	7.95	0.40	0.255	0.012	0.96	0.2263	0.0063	2225	113	1463	64	3026	22	48
Zircon 48	1531	199	0.14	2.38	0.12	0.130	0.006	0.96	0.1330	0.0039	1237	64	788	36	2138	25	37
Zircon 49	1927	270	0.03	2.43	0.12	0.140	0.007	0.96	0.1257	0.0036	1251	64	846	39	2038	25	42
Zircon 50	1360	190	0.19	2.71	0.14	0.140	0.007	0.96	0.1406	0.0041	1330	69	842	39	2235	25	38
Zircon 51	1496	330	0.02	5.92	0.30	0.221	0.011	0.96	0.1944	0.0055	1964	101	1286	57	2780	23	46
Zircon 52	577	187	0.37	9.99	0.53	0.324	0.016	0.95	0.2236	0.0071	2434	129	1809	80	3007	25	60
Zircon 53	874	302	0.41	10.58	0.55	0.346	0.017	0.96	0.2220	0.0063	2487	128	1914	82	2996	23	64
Zircon 54	1819	322	0.02	3.94	0.20	0.177	0.009	0.96	0.1614	0.0046	1622	84	1051	48	2470	24	43
Zircon 55	1893	252	0.05	2.45	0.13	0.133	0.007	0.96	0.1335	0.0039	1258	65	807	38	2144	26	38
Zircon 59	1226	354	0.71	7.11	0.37	0.289	0.015	0.96	0.1786	0.0055	2125	112	1635	73	2640	25	62
Zircon 60	812	310	0.71	10.72	0.57	0.382	0.019	0.96	0.2034	0.0063	2499	132	2087	90	2853	25	73

Table 2. Continued

Analysis	U [a] (ppm)	Pb [a] (ppm)	Th/U [a]	$^{207}Pb/^{235}U$ [b]	2 σ [d]	$^{206}Pb/^{238}U$ [b]	2 σ [d]	rho [c]	$^{207}Pb/^{206}Pb$ [e]	2 σ [d]	$^{207}Pb/^{235}U$	2 σ	$^{206}Pb/^{238}U$	2 σ	$^{207}Pb/^{206}Pb$ (Ma)	2 σ	%
Zircon 61	1099	263	0.33	6.43	0.34	0.240	0.012	0.95	0.1945	0.0062	2036	108	1385	63	2780	26	50
Zircon 62	739	180	0.52	6.68	0.36	0.243	0.012	0.95	0.1995	0.0066	2070	111	1402	65	2822	27	50
Zircon 63	2211	378	0.02	3.79	0.20	0.171	0.009	0.96	0.1610	0.0050	1591	84	1017	48	2466	26	41
Zircon 64	2188	208	0.16	1.86	0.10	0.095	0.005	0.95	0.1420	0.0048	1067	58	585	29	2252	29	26
Zircon 65	894	291	0.50	10.65	0.57	0.325	0.017	0.95	0.2377	0.0078	2493	135	1814	81	3105	26	58
Zircon 66	1473	224	0.02	2.99	0.16	0.152	0.008	0.95	0.1424	0.0049	1405	76	914	44	2257	30	40
Zircon 67	2016	270	0.02	2.27	0.12	0.134	0.007	0.95	0.1226	0.0040	1202	65	811	39	1995	29	41
Zircon 72	2126	438	0.03	7.28	0.40	0.206	0.011	0.95	0.2566	0.0088	2147	118	1207	57	3226	27	37
Zircon 73	585	228	0.28	10.64	0.59	0.391	0.021	0.94	0.1975	0.0072	2492	139	2126	95	2806	30	76
Zircon 74	2878	451	0.03	2.98	0.16	0.157	0.008	0.95	0.1379	0.0048	1401	77	938	45	2201	30	43
Zircon 75	1614	273	0.07	4.01	0.22	0.169	0.009	0.95	0.1715	0.0061	1635	90	1009	49	2573	29	39
Zircon 76	1252	270	0.18	5.43	0.30	0.216	0.011	0.95	0.1823	0.0065	1889	105	1261	60	2674	29	47

[a]U and Pb concentrations and Th/U ratios are calculated relative to the GJ-1 reference zircon
[b]Corrected for background and within-run Pb/U fractionation and normalized to reference zircon GJ-1 (ID-TIMS values/measured value); $^{207}Pb/^{235}U$ calculated using $(^{207}Pb/^{206}Pb)/(^{238}U/^{206}Pb * 1/137.88)$
[c]Rho is the error correlation defined as the quotient of the propagated errors of the $^{206}Pb/^{238}U$ and the $^{207}Pb/^{235}U$ ratios
[d]Quadratic addition of within-run errors (2 s.d.) and daily reproducibility of GJ-1 (2 s.d)
[e]Corrected for mass-bias by normalizing to the GJ-1 reference zircon (~ 0.6 per atomic mass unit) and common Pb using the model Pb composition of Stacey & Kramers (1975)

and lower intercept ages (532 ± 76 Ma) with a very high MSWD of 91, indicating that the dataset cannot be explained with a single lead-loss event and has excess scatter that is pointing to a petrogenetic evolution with multiple lead-loss events (Mezger & Krogstad, 1997; Corfu, 2012; Kröner *et al.* 2014). Nevertheless, we suggest that the ^{207}Pb–^{206}Pb age of the more concordant analysis (~ 3.44 Ga) may indicate the intrusion age for the protolith of the TTG gneiss DUR13.

5. Lu–Hf zircon data

5.a. Lu–Hf methodology

Hafnium isotope measurements were performed with a Thermo Finnigan NEPTUNE multi-collector ICP-MS at Goethe University Frankfurt (GUF) coupled to a RESOlution M50 193 nm ArF excimer (Resonetics) laser system following the method described in Gerdes & Zeh (2006, 2009). Spots of 40 µm in diameter were drilled with a repetition rate of 5.5 Hz and an energy density of 6 J cm^{-2} during 40 seconds of data acquisition. Accuracy and external reproducibility of the method was verified by repeated analyses of reference zircons GJ-1 and Plešovice, which yielded $^{176}Hf/^{177}Hf$ of 0.282010 ± 0.000025 (2 s.d., n = 7) and 0.0282475 ± 0.000020 (n = 7), respectively. This is in perfect agreement with previously published results (e.g. Gerdes & Zeh, 2006; Sláma *et al.* 2008) and with the LA-MC-ICP-MS seven-year long-term averages for the GJ-1 (0.282010 ± 0.000024; n > 900) and Plešovice (0.282478 ± 0.000023, n > 500) reference zircons at GUF.

The initial $^{176}Hf/^{177}Hf$ values are expressed as εHf(t), which is calculated using a decay constant value of $1.867 \times 10{-}11$ $year^{-1}$, CHUR after Bouvier, Vervoort & Patchett (2008; $^{176}Hf/^{177}Hf_{CHUR,today}$ = 0.282785 and $^{176}Lu/^{177}Hf_{CHUR,today}$ = 0.0336) and the Pb–Pb ages obtained from the upper intercept ages of two zircon populations (method discussed by Corfu, 2012). For the calculation of Hf two-stage model ages (T_{DM}) in billions of years the measured $^{176}Lu/^{177}Hf$ of each spot (first stage = age of zircon), a value of 0.0113 for the average continental crust and a depleted mantle (DM) $^{176}Lu/^{177}Lu_{DM}$ = 0.0384 and $^{176}Hf/^{177}Hf_{DM}$ = 0.283165 (average MORB; Chauvel *et al.* 2008) were used.

5.b. Zircon Lu–Hf analyses of LB13

As discussed by Fisher *et al.* (2014), in the case of multiple zircon populations in any ancient rock, it is important to verify whether zircons represent single or mixed generations. Figure 3c and also the Terra-Wasserburg Concordia plot in the online Supplementary Material (available at http://journals.cambridge.org/geo) show that the two zircon populations of LB13 (~ 3.59 Ga and 3.44 Ga) occur as separate age groups without evidence of mixing. So it is concluded that the zircon ages in LB13 reflect two distinct crystallization events, and initial εHf(t) values have been calculated for each age group on the basis of their respective upper intercept ages.

Zircons with an apparent Pb–Pb age of ~ 3.44 Ga yield $^{176}Hf/^{177}Hf$ of 0.280539 to 0.280592 corresponding to εHf(t) values of −0.6 to +1.3 (Table 3). A T_{DM} model age of ~ 3.55 Ga obtained from the ~ 3.44 Ga zircons and near-chondritic average $\varepsilon Hf_{3.44Ga}$ (+0.3) indicates that the calc-alkaline magma was formed by partial melting of a 3.55 Ga mafic crust. The analyses of the older zircon population (~ 3.59 Ga) of TTG gneiss LB13 yield $^{176}Hf/^{177}Hf$ of 0.280524 to 0.280496 corresponding to εHf(t) values of +2.4

https://doi.org/10.1017/S0016756815000692 Published online by Cambridge University Press

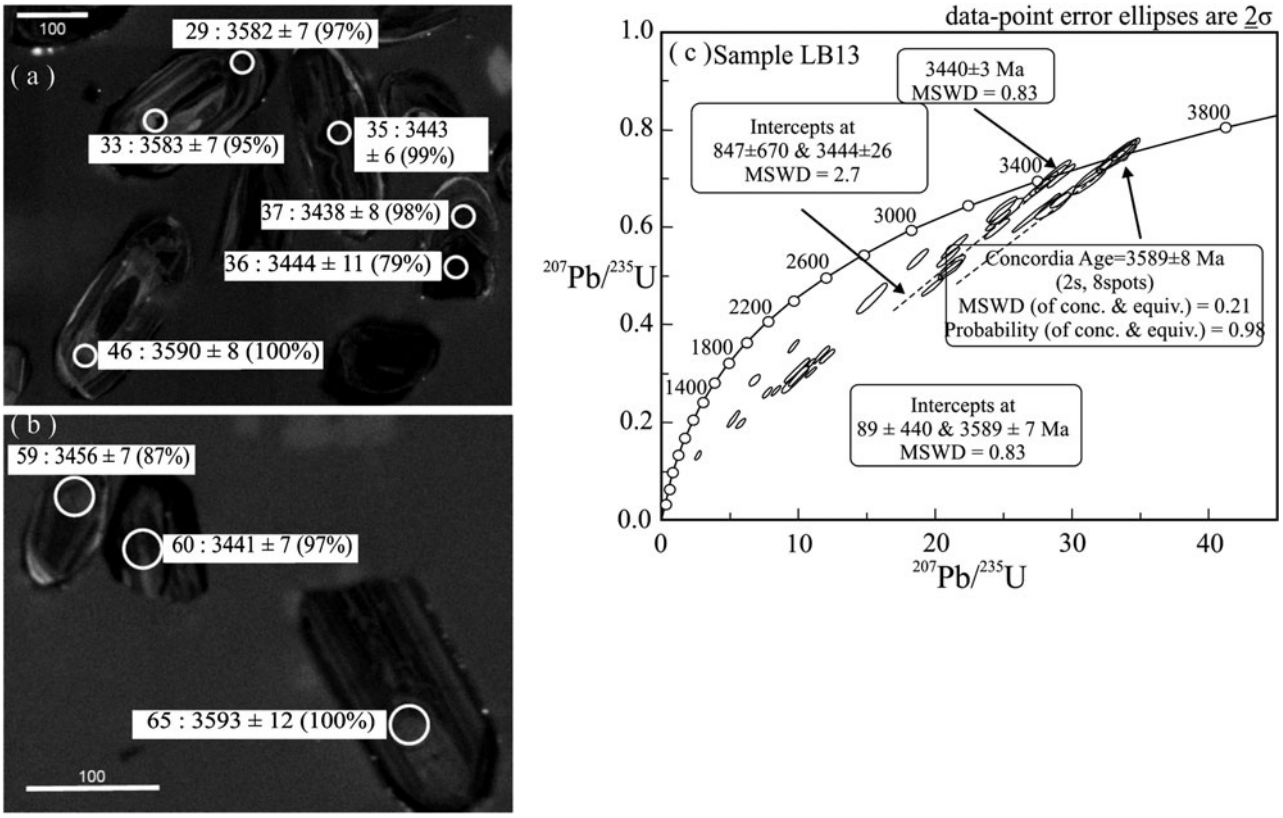

Figure 3. (a, b) CL images of zircons from sample LB13. The position of the laser spots (30 μm in diameter) is indicated by white circles. Labels indicate analysis number, the estimated ^{207}Pb–^{206}Pb ages with 2σ errors (in Ma) and the degree of concordance (in %). (c) Concordia diagram showing the laser ablation analyses of zircons of two distinct age groups (3.59 Ga and 3.44 Ga).

to +1.4. Average $\varepsilon Hf_{3.59Ga}$ values (+1.9) of the older zircon population are more suprachondritic, indicating influence of depleted mantle (Table 3; Fig. 5).

6. Discussion: Palaeoarchaean crustal evolution of the central part of the Bundelkhand Craton

Our study reports zircon ages (magmatic) of ~ 3.44 Ga from the TTG gneiss (LB13) of the Babina area from the western part of the Bundelkhand Tectonic Zone (Table 1; Fig. 3c). These TTG gneisses are dominantly composed of sodic plagioclase, quartz, biotite, hornblende and chlorite. T_{DM} model ages (~ 3.55 Ga) and near-chondritic εHf (−0.6 to +1.3) values of the zircons indicate an origin of the calc-alkaline magma from melting of a ~ 3.55 Ga mafic crust. A set of older zircons from the gneiss yield a Pb–Pb age of ~ 3.59 Ga (Table 1; Fig. 3c). Average εHf values of these zircons are more suprachondritic (+1.9). The ages of these zircons are similar to the crystallization age (~ 3.56 Ga) of the trondhjemite gneiss from the Mauranipur area of the central Bundelkhand Craton. It is, therefore, concluded that the older zircons (~ 3.59 Ga) represent xenocrystic zircons from a pre-existing felsic crust. Reports of older zircon xenocrysts in TTGs have been made by Acharyaa, Gupta & Orihashi (2010) from the 3.45 Ga Singhbhum Granite and also by Kröner *et al.* (2012) from the Ancient Gneiss Complex in Swaziland. More discordant ages have been obtained from the zircons of the TTG gneiss DUR13 in the study area (Table 2; Fig. 4c). A sole concordant age of ~ 3.44 Ga obtained from the sample indicates that the ~ 3.44 Ga TTG gneisses in the study area have been strongly metamorphosed and possibly re-melted (as observed from multiple melt or leucocratic phases in Fig. 2c, d) during later tectonothermal events.

A chronological correlation between the Palaeo- to Mesoarchaean crustal components of the Bundelkhand Craton with other Archaean cratons in peninsular India is given in Table 4. The present study thus indicates that crust-forming processes in the central Bundelkhand Craton initiated at ~ 3.59 Ga, a time-period much older than that of ~ 3.3 Ga as proposed by Mondal *et al.* (2002) (Table 4). A second phase of calc-alkaline magmatism occurred in this part of the craton at ~ 3.44 Ga (Table 4).The correlation indicates that the ~ 3.59 Ga zircon age obtained from the Babina TTG gneiss and that obtained from the Mauranipur area by Kaur, Zeh & Chaudhri (2014) are similar to that recorded from the TTG gneiss and granites from the central part of the Bastar Craton in central India, the felsic volcanic rocks from the Iron Ore Group and the detrital zircons from the Older Metamorphic Group of the Singhbum Craton in eastern India and the Sargur supracrustal rocks from the Dharwar Craton, southern India (Nutman *et al.* 1992; Ghosh, 2004; Mukhopadhyay *et al.* 2008; Rajesh *et al.* 2009). The ~ 3.44 Ga age of TTG magmatism recorded from the central part of the Bundelkhand Craton can also be correlated with the time-frame of crystallization of the Older Metamorphic Tonalitic Gneiss and Singhbhum Granite-I in the Singhbhum Craton, and the age of the detrital zircons obtained from supracrustal sequences of the Sargur Group in the Western Dharwar Craton (Mishra *et al.* 1999; Maibam, Goswami & Srinivasan, 2011; Table 4). Thus, the

https://doi.org/10.1017/S0016756815000692 Published online by Cambridge University Press

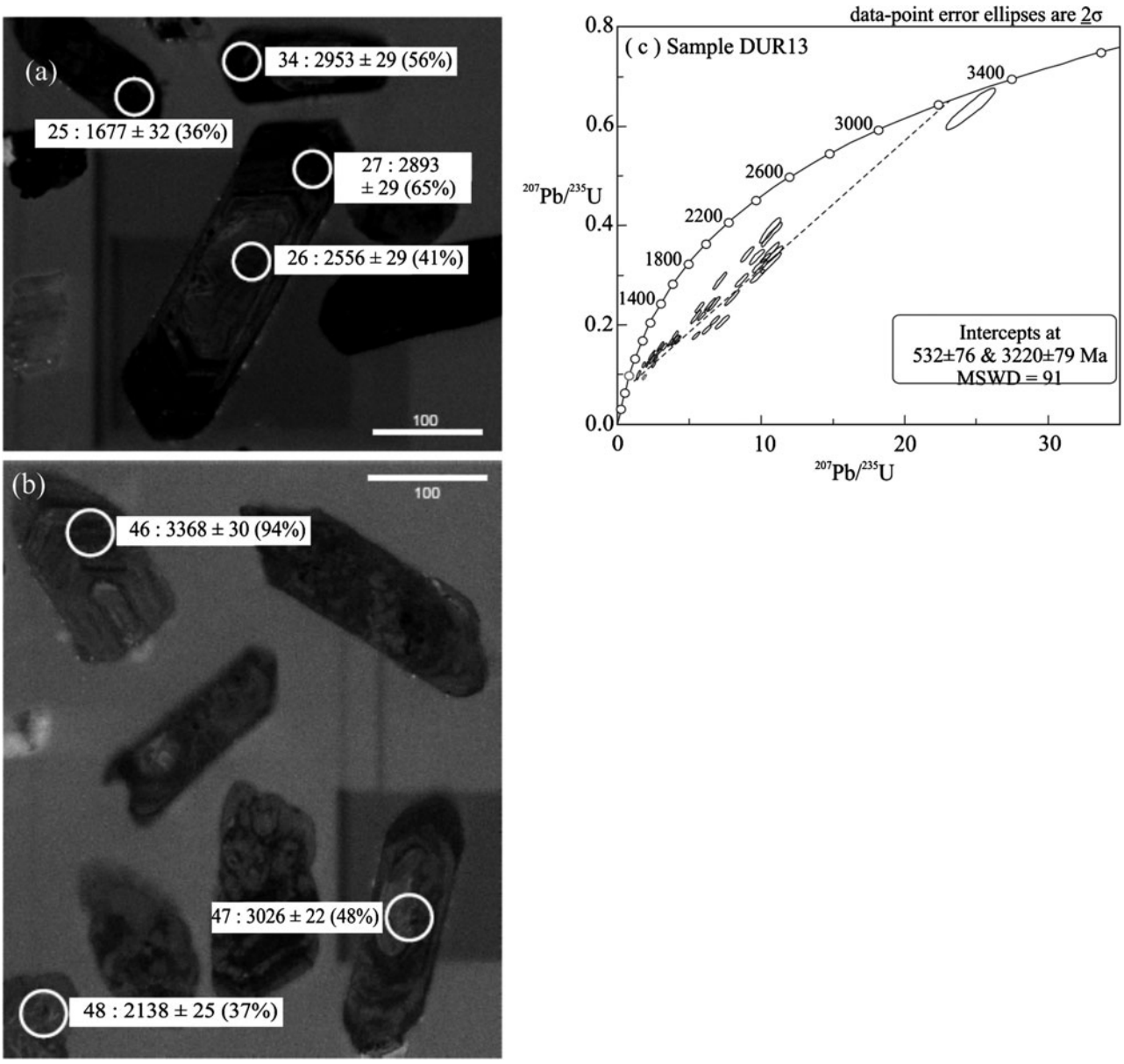

Figure 4. (a, b) CL images of zircons from sample DUR13. The position of the laser spots (30 μm in diameter) is indicated by white circles. Labels indicate analysis number, the estimated ^{207}Pb–^{206}Pb ages with 2σ errors (in Ma) and the degree of concordance (in %). (c) Concordia diagram showing the laser ablation zircon analyses, most of the zircons showing strong discordance with an upper intercept at ~ 3.22 Ga and one concordant analysis yielding an age of ~ 3.36 Ga.

crust-forming process in the Bundelkhand Craton initiated in the same time-frame (~ 3.6 Ga) as that recorded from the Bastar and Singhbhum cratons, a time-frame when continental crust formation became widespread throughout the world, as seen in the representative sketch of the Ur Supercontinent in Figure 6. A major episode of tectonothermal activity is recorded in the Bundelkhand Craton at ~ 3.44 Ga and this has so far been recorded only from the Singhbhum Craton. Therefore, it is possible that the North Indian Shield cratons had similar Palaeoarchaean tectonothermal histories. The similar Palaeoarchaean time-frames for the evolution of the Bundelkhand, Bastar and Singhbhum cratons is support for the Bundelkhand Craton being part of the Ur Supercontinent (Fig. 6). Discordant data from the TTG gneiss show three major peaks at ~ 3.0–2.8 Ga, 2.6–2.5 Ga and 2.2–2.0 Ga, indicating lead-loss events that can be correlated, respectively, with high-pressure metamorphism, large-scale granite magmatism and intrusion of mafic dyke swarms, reported from the craton.

Acknowledgements. LS acknowledges the Competitive Research Grant (2010-2012) sponsored by the University of KwaZulu-Natal, Durban, South Africa for providing funding for the field work in Bundelkhand Craton. DF acknowledges Fundisile Nkumenge for performing zircon separation and sample preparation. JKP acknowledges GRBM Project, Ministry of Environment and Forest, Govt. of India for providing funding for field work. PN acknowledges the Director, IISER Bhopal, for providing funding for conducting field work. The authors also acknowledge Kåre Kullerud and Allen Nutman for their suggestions to improve the scientific contents of the manuscript. Technical help from Prof. Fernando Corfu is gratefully acknowledged to improve the scientific content and restructuring of the manuscript.

Supplementary material

To view supplementary material for this article, please visit http://dx.doi.org/10.1017/S0016756815000692

Table 3. LA-MC-ICP-MS Lu–Hf isotope data for zircons from TTG gneiss (LB13) from the Babina area

	$^{176}Yb/^{177}Hf$ [a]	±2σ	$^{176}Lu/^{177}Hf$ [a]	±2σ	$^{178}Hf/^{177}Hf$	$^{180}Hf/^{177}Hf$	Sig_{Hf} [b] (V)	$^{176}Hf/^{177}Hf$	±2σ [c]	$^{176}Hf/^{177}Hf_{(t)}$ [d]	εHf(t) [d]	±2σ [c]	T_{DM} [e] (Ga)	Age [f] (Ma)	±2σ
LB13-29	0.0271	0	0.00087	0	1.46730	1.88699	11	0.280569	0	0.280509	1.9	0.8		3582	7
LB13-33	0.0243	0	0.00090	0	1.46726	1.88669	9	0.280570	0	0.280508	1.8	1.0		3583	7
LB13-46	0.0067	0	0.00027	0	1.46720	1.88652	6	0.280542	0	0.280524	2.4	1.3		3590	7
LB13-48	0.0502	0	0.00156	0	1.46728	1.88684	14	0.280612	0	0.280504	1.7	0.8		3583	7
LB13-50	0.0767	0	0.00241	0	1.46729	1.88672	14	0.280662	0	0.280496	1.4	0.8		3549	8
LB13-27	0.0216	0	0.00078	0	1.46713	1.88671	11	0.280602	0	0.280550	− 0.2	1.0	3.53	3380	5
LB13-34	0.0401	0	0.00140	0	1.46727	1.88695	13	0.280631	0	0.280534	− 0.6	0.8	3.55	3411	5
LB13-37	0.0318	0	0.00113	0	1.46716	1.88677	8	0.280666	0	0.280592	1.3	0.9	3.44	3438	11
LB13-49	0.0140	0	0.00052	0	1.46715	1.88671	14	0.280575	0	0.280540	− 0.6	1.0	3.54	3471	14
LB13-53	0.0183	0	0.00069	0	1.46726	1.88671	11	0.280622	0	0.280576	0.7	1.0	3.47	3419	8
LB13-59	0.0429	0	0.00144	0	1.46727	1.88685	10	0.280688	0	0.280592	1.3	0.8	3.44	3456	6
LB13-61	0.0354	0	0.00124	0	1.46729	1.88688	8	0.280641	0	0.280559	0.1	1.0	3.51	3438	6
LB13-62	0.0448	0	0.00157	0	1.46730	1.88689	13	0.280667	0	0.280563	0.2	0.9	3.50	3462	7
Plešovice (n = 7)	0.0055	32	0.00014	8	1.46730	1.88670	14	0.282476	20	0.282475	− 3.4	0.7	1.17	338	3
GJ-1 (n = 7)	0.0076	6	0.00026	0	1.46729	1.88671	9	0.282013	25	0.282010	− 3.9	0.9	1.96	606	6
JMC 475 (n = 6)					1.46719	1.88669	11	0.282149	8						

Quoted uncertainties (absolute) relate to the last quoted figure. The effect of the inter-element fractionation on the Lu/Hf was estimated to be about 6 % or less based on analyses of the GJ-1 and Plešovice zircons. Accuracy and reproducibility were checked by repeated analyses (n = 7) of reference zircon GJ-1 and Plesoviče (data given as mean with 2 standard deviation uncertainties)

(a) $^{176}Yb/^{177}Hf = (^{176}Yb/^{173}Yb)_{true} \times (^{173}Yb/^{177}Hf)_{meas} \times (M_{173(Yb)}/M_{177(Hf)})^{b(Hf)}$, $b(Hf) = \ln(^{179}Hf/^{177}Hf_{true} / {}^{179}Hf/^{177}Hf_{measured})/ \ln (M_{179(Hf)}/M_{177(Hf)})$, M = mass of respective isotope. The $^{176}Lu/^{177}Hf$ were calculated in a similar way by using the $^{175}Lu/^{177}Hf$.

(b) Mean Hf signal in volts

(c) Uncertainties are quadratic additions of the within-run precision and the daily reproducibility of the 40 ppb-JMC475 solution. Uncertainties for the JMC475 quoted at 2 s.d.

(d) Initial $^{176}Hf/^{177}Hf$ and εHf calculated using the apparent Pb–Pb age determined by LA-ICP-MS dating (see column f), and the CHUR parameters: 176Lu/^{177}Hf = 0.0336 and $^{176}Hf/^{177}Hf$ = 0.282785 (Bouvier, Vervoort & Patchett, 2008)

(e) Two-stage model age in billions of years using the measured $^{176}Lu/^{177}Hf$ of each spot (first stage = age of zircon), a value of 0.0113 for the average continental crust (second stage) and a depleted mantle (DM<, Chauvel *et al.* 2008) $^{176}Lu/^{177}Hf$ and $^{176}Hf/^{177}Hf$ of 0.0384 and 0.28316, respectively.

(f) Apparent Pb–Pb age determined by LA-ICP-MS

Table 4. Correlation of Palaeo–Mesoarchaean crustal components of the Bundelkhand Craton with that recorded from other Archaean cratons of peninsular India

	Bundelkhand Craton	Aravalli Craton	Singhbhum Craton	Bastar Craton	Western Dharwar Craton	Eastern Dharwar Craton
2.8–2.5 Ga	High-pressure metamorphism, felsic magmatism (Saha *et al.* 2011; Mondal *et al.* 2002)	Crystallization ages of Banded Gneissic Complex, Berach Granite (Roy *et al.* 2012)	Crystallization ages of the Mayur Bhanj Granite, eastern and western margins of the Singhbhum Craton (Saha *et al.* 1977; Mishra *et al.* 1999; Bandyopadhyay *et al.* 2001).	Not recorded	Supracrustal sequence and potassic granite (Meen, Rogers & Fullagar, 1992; Nutman *et al.* 1992, 1996; Peucat, Mahabaleshwar & Jayananda, 1993; Peucat *et al.* 1995; Ramakrishnan, Venkatadasu & Kröner, 1994).	TTG magmatism and intrusion of potassic granite (Jayananda *et al.* 2000)
3.2–3.0 Ga	U–Pb zircon ages recorded from the TTG gneiss in the Sukwan-Dukwan dam area and near Panchwara (present study; Mondal *et al.* 2002).	U–Pb zircon ages from the Alwar quartzite of the Aravalli Supergroup (Kaur *et al.* 2011).	U–Pb zircon overgrowth in the magmatic zircons from the Older Metamorphic Tonalitic Gneiss and detrital zircons from the Older Metamorphic Group (Mishra *et al.* 1999)	Not recorded	Pb–Pb zircon ages obtained from the TTG gneisses of the Nuggihalli schist belt and an orthogneiss clast in the Kaladurga conglomerate (Maibam, Goswami & Srinivasan, 2011)	Pb–Pb zircon age from the Sakarsanhalli TTG gneiss (Maibam, Goswami & Srinivasan, 2011)
3.3 Ga	Pb–Pb zircon ages from Kuraicha and Mahoba gneisses; Pb–Pb zircon age from a metabasic enclave in the Mahoba Gneiss (Mondal *et al.* 2002)	Whole-rock Sm–Nd and Pb–Pb zircon ages from the Mewar Gneiss (Gopalan *et al.* 1990; Wiedenbeck & Goswami, 1994); U–Pb detrital zircon ages from the Alwar quartzite of the Aravalli Supergroup (Kaur *et al.* 2011)	Pb–Pb zircon ages from the Singhbum Granite-II (Mishra *et al.* 1999)	Not recorded	U–Pb zircon ages from the Gorur gneiss (Beckinsale, Drury & Holt, 1980; Peucat, Mahabaleshwar & Jayananda, 1993); U–Pb zircon ages from the meta-rhyolite of the Holenarsipur supracrustal units (Peucat *et al.* 1995); whole-rock Sm–Nd isochron age from komatiite of the Sargur supracrustal unit (Jayananda *et al.* 2008).	Pb–Pb zircon age from the Hulimavu orthogneiss (Maibam, Goswami & Srinivasan, 2011)
3.4 Ga	U–Pb zircon age from Babina TTG gneiss (present study)	Not recorded	Pb–Pb zircon ages from the Older Metamorphic Tonalite Gneiss and Singhbhum granite Phase-I (Mishra *et al.* 1999; Acharyaa, Gupta & Orihashi, 2010)	Not recorded	Pb–Pb detrital zircon ages from the Sargur supracrustal units (Maibam, Goswami & Srinivasan, 2011)	Not recorded
3.6–3.5 Ga	U–Pb zircon age from Babina TTG gneiss (present study; Kaur, Zeh & Chaudhri, 2014); Whole-rock Rb–Sr from Baghora gneiss south of Babina (Sarkar, Paul & Potts, 1996)	Not recorded	U–Pb zircon ages from the felsic volcanics of the Iron Ore Group (Mukhopadhyay *et al.* 2008); Pb–Pb detrital zircon ages from the Older Metamorphic Group (Goswami *et al.* 1995; Mishra *et al.* 1999).	U–Pb zircon ages from TTG gneiss and granite (Ghosh, 2004; Rajesh *et al.* 2009)	U–Pb detrital zircon ages from the Sargur supracrustal units (Nutman *et al.* 1992)	Not recorded

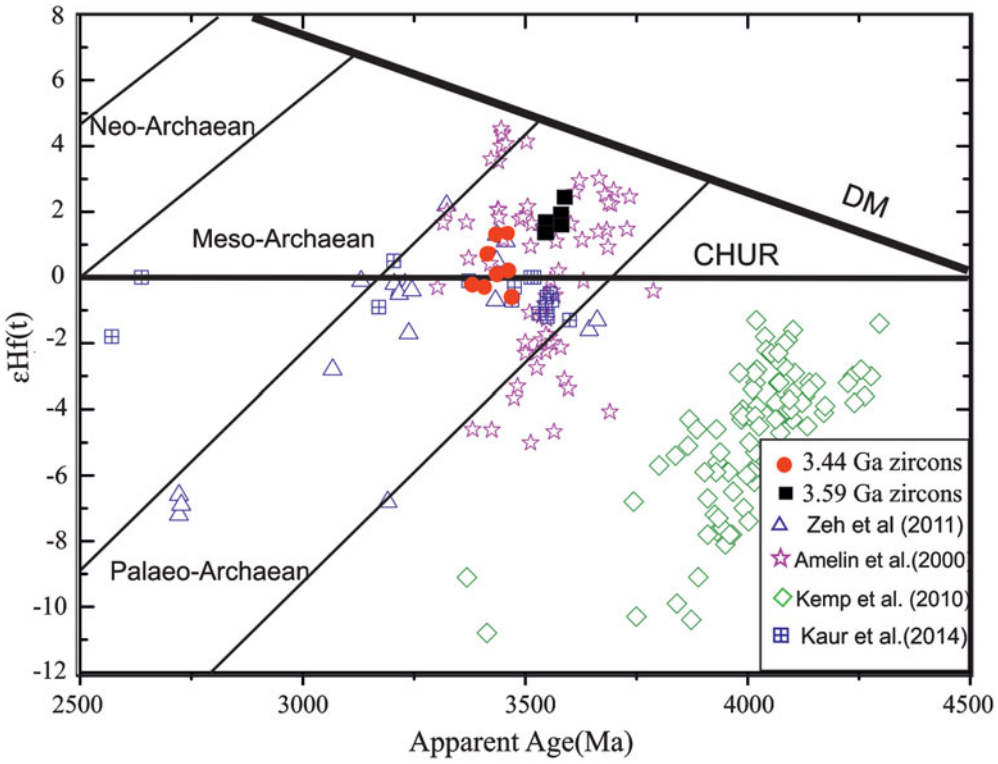

Figure 5. (Colour online) Hf isotope data displayed in the εHf(t) versus U–Pb age diagram of zircons from TTG gneiss sample LB13. Symbols represent analysis of individual growth domains of zircons from the different samples. Shown for comparison are the depleted mantle (Chauvel *et al.* 2008) and the fields of the Neoarchaean to Palaeoarchaean crust, assuming a crustal $^{176}Lu/^{177}Hf$ of 0.0113. Hf isotope data from the Archaean zircons of the Ancient Gneissic Complex, Swaziland (Zeh, Gerdes & Millonig, 2011), Acasta Gneiss Complex, Barberton Belt, Pilbara Craton (Amelin, Lee & Halliday, 2000), Zack Hills, Australia (Kemp *et al.* 2010) and Mauranipur area of the Bundelkhand Craton (Kaur, Zeh & Chaudhri, 2014) are also shown.

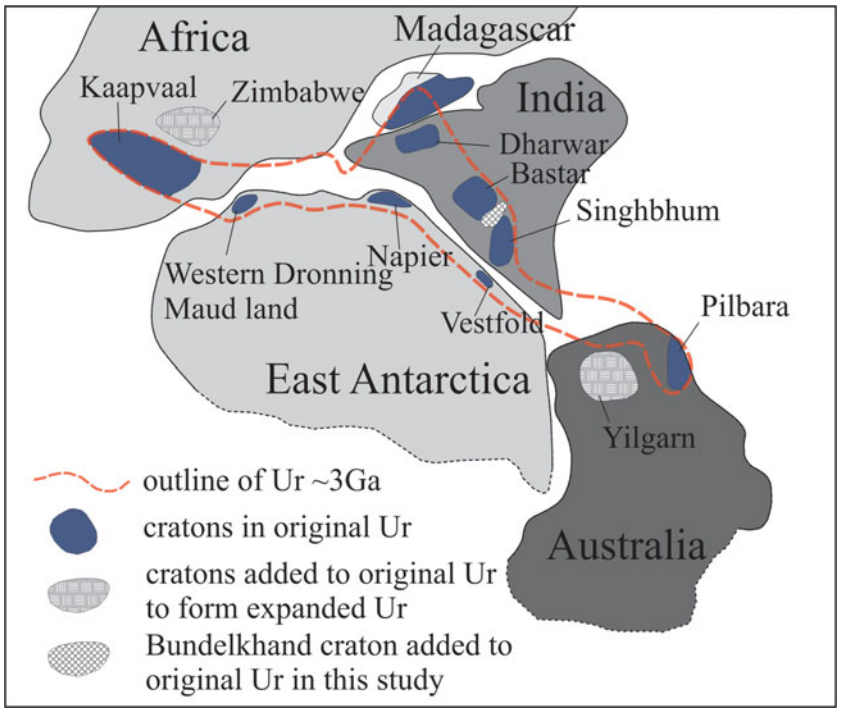

Figure 6. (Colour online) Schematic diagram showing position of the Bundelkhand Craton in the Ur Supercontinent (after Rogers, 1996) that may explain the similar crust-forming processes in the Palaeo–Mesoarchaean.

https://doi.org/10.1017/S0016756815000692 Published online by Cambridge University Press

References

ACHARYAA, S. K., GUPTA, A. & ORIHASHI, Y. 2010. New U–Pb zircon ages from Paleo–Mesoarchean TTG gneisses of the Singhbhum Craton, Eastern India. *Geochemical Journal* **44**, 81–8.

AMELIN, Y., LEE, D.-C. & HALLIDAY, A. N. 2000. Early-middle Archaean crustal evolution deduced from Lu–Hf and U–Pb isotopic studies of single zircon grains. *Geochimica Cosmochimica Acta* **64**, 4205–25.

BANDYOPADHYAY, P. K., CHAKRABARTI, A. K., DEOMURARI, M. P. & MISRA, S. 2001. 2.8 Ga old anorogenic granite-acid volcanic association from western margin of Singhbhum–Orissa craton, eastern India. *Gondwana Research* **4**, 465–75.

BASU, A. K. 1986. Geology of parts of Bundelkhand granite massif, central India. *Record of the Geological Survey of India* **11**, 61–124.

BECKINSALE, R. D., DRURY, S. A. & HOLT, R. W. 1980. 3300-Myr old gneisses from the South Indian Craton. *Nature* **283**, 469–70.

BOUVIER, A., VERVOORT, J. & PATCHETT, P. 2008. The Lu–Hf and Sm–Nd isotopic composition of CHUR: constraints from unequilibrated chondrites and implications for the bulk composition of terrestrial planets. *Earth and Planetary Science Letters* **273**, 48–57.

CHAUVEL, C., LEWIN, E., CARPENTIER, M., ARNDT, N. T. & MARINI, J. 2008. Role of recycled oceanic basalt and sediment in generating the Hf–Nd mantle array. *Nature Geoscience* **1**, 64–7.

CONDIE, K. C. 2000. Episodic continental growth models: afterthoughts and extensions. *Tectonophysics* **322**, 153–62.

CORFU, F. 2012. A century of U–Pb geochronology: the long quest towards concordance. *Geological Society of America Bulletin* **125**, 33–47.

FISHER, C. M., VERVOORT, J. D. & HANCHAR, J. M. 2014. Guidelines for reporting zircon Hf isotope data by LA-MC-ICPMS and potential pitfalls in the interpretation of these data. *Chemical geology* **363**, 125–33.

FREI, D. & GERDES, A. 2009. Precise and accurate in situ U–Pb dating of zircon with high sample throughput by automated LA-SF-ICPMS. *Chemical Geology* **261**, 261–70.

FRIEND, C. R. L. & NUTMAN, A. P. 2005. Complex 3670–3500 Ma orogenic episodes superimposed on juvenile crust accreted between 3850 and 3690 MA, Itsaq Gneiss Complex, southern West Greenland. *Journal of Geology* **113**, 375–97.

GERDES, A. & ZEH, A. 2006. Combined U–Pb and Hf isotope LA-(MC)-ICP-MS analyses of detrital zircons: comparison with SHRIMP and new constraints for the provenance and age of an Armorican metasediment in Central Germany. *Earth and Planetary Science Letters* **249**, 47–61.

GERDES, A. & ZEH, A. 2009. Zircon formation versus zircon alteration — new insights from combined U–Pb and Lu–Hf in-situ LA-ICP-MS analyses, and consequences for the interpretation of Archean zircon from the Central Zone of the Limpopo Belt. *Chemical Geology* **261**, 230–43.

GHOSH, J. G. 2004. 3.56 Ga tonalite in the central part of the Bastar craton, India: oldest Indian date. *Journal of Asian Earth Science* **23**, 359–64.

GOPALAN, K., MACDOUGALL, J. D., ROY, A. B. & MURALI, A. V. 1990. Sm–Nd evidence for 3.3 Ga old rock in Rajasthan, north-western India. *Precambrian Research* **48**, 287–97.

GOSWAMI, J. N., MISRA, S., WIEDENBACK, M., RAY, S. L. & SAHA, A. K. 1995. 3.55 Ga-old zircon from Singhbhum-Orissa Iron Ore craton, eastern India. *Current Science* **69**, 1008–11.

HARRISON, T., SCHMITT, A., MCCULLOCH, M. & LOVERA, O. 2008. Early (>4.5 Ga) formation of terrestrial crust: Lu-Hf, δ18O, and Ti thermometry results for Hadean zircons. *Earth and Planetary Science Letters* **268**, 476–86.

IIZUKA, T., KOMIYA, T., UENO, Y., KATAYAMA, I., UEHARA, Y., MARUYAMA, S., HIRATA, T., JOHNSON, S. P. & DUNKLEY, D. J. 2007. Geology and zircon geochronology of the Acasta Gneiss Complex, northwestern Canada: new constraints on its tectonothermal history. *Precambrian Research* **153**, 179–208.

JAYANANDA, M., KANOB, T., PEUCAT, J.-J. & CHANNABASAPPA, S. 2008. 3.35 Ga komatiite volcanism in the western Dharwar craton, southern India: constraints from Nd isotopes and whole-rock geochemistry. *Precambrian Research* **162**, 160–79.

JAYANANDA, M., MOYEN, J.-F., MARTIN, H., PEUCAT, J.-J., AUVRAY, B. & MAHABALESWAR, B. 2000. Late Archean (2550–2520 Ma) juvenile magmatism in the Eastern Dharwar craton, southern India: constraints from geochronology, Nd–Sr isotopes and whole rock geochemistry. *Precambrian Research* **99**, 225–54.

KAUR, P., ZEH, A., CHAUDHRI, N., GERDES, A. & OKRUSCH, M. 2011. Archaean to Palaeoproterozoic crustal evolution of the Aravalli mountain range, NW India, and its hinterland: the U–Pb and Hf isotope record of detrital zircon. *Precambrian Research* **187**, 155–164.

KAUR, P., ZEH, A. & CHAUDHRI, N. 2014. Characteristic of U–Pb–Hf isotope record of the 3.55 Ga felsic crust from the Bundelkhand Craton, Northern India. *Precambrian Research* **255**, 236–44.

KEMP, A. I. S., WILDE, S. A., HAWKESWORTH, C. J., COATH, C. D., NEMCHIN, A. & PIDGEON, R. T. 2010. Hadean crustal evolution revisited: new constraints from Pb–Hf isotope systematics of the Jack Hills zircons. *Earth and Planetary Science Letters* **296**, 45–56.

KRÖNER, A., HOFMANN, J., XIE, H., WU, F., MÜNKER, C., HEGNER, E., WONG, J., WAN, Y. & LIU, D. 2012. Generation of early Archean felsic volcanics and TTG gneisses through crustal melting, eastern Kaapvaal craton, southern Africa. American Geophysical Union Fall Meeting 2012, abstract #T14B-08.

KRÖNER, A., WAN, A., LIU, X. & LIU, D. 2014. Dating of zircon from high-grade rocks: which is the most reliable method? *Geoscience Frontiers* **5**, 515–23.

KUMAR, S., YI, K., RAJU, K., PATHAK, M., KIM, N. & LEE, T. H. 2011. SHRIMP U–Pb geochronology of felsic magmatic lithounits in the central part of Bundelkhand Craton, Central India. In *7th Hutton Symposium on Granites and Related Rocks* (eds J. F. Molina, J. H. Scarrow, F. Bea & P. Montero), p. 83.

LUDWIG, K. 2003. *Isoplot/Ex Version 3: A Geochronological Toolkit for Microsoft Excel*. Berkeley Geochronology Center Special Publication 1, 43 pp.

MAIBAM, B., GOSWAMI, J. N. & SRINIVASAN, R. 2011. Pb–Pb zircon ages of Archean metasediments and gneisses from the Dharwar craton, southern India: implications for the antiquity of the eastern Dharwar craton. *Journal of Earth System Sciences* **120**, 643–61.

MALVIYA, V. P., ARIMA, M. & PATI, J. K. 2005. Island arc related Archean mafic volcanism from Bundelkhand craton, Central India – an implication from Nd model ages. Abstracts, Joint Meeting of Earth and Planetary Sciences, Japan.

MATTINSON, J. M. 2010. Analysis of the relative decay constants of ^{235}U and ^{238}U by multi-step CA-TIMS measurements of closed-system natural zircon samples. *Chemical Geology* **275**, 186–98.

MEEN, J. K., ROGERS, J. J. W. & FULLAGAR, P. D. 1992. Lead isotopic composition in the western Dharwar craton, southern India: evidence for distinct middle Archaean terrains in a late Archaean craton. *Geochimica Cosmochimica Acta* **56**, 2455–70.

MEERT, J. G., PANDIT, M. K., PRADHAN, V. R., BANKS, J., SIRIANNI, R., STROUD, M., NEWSTEAD, B. & GIFFORD, J. 2010. Precambrian crustal evolution of Peninsular India: a 3.0 billion year odyssey. *Journal of Asian Earth Sciences* **39**, 483–515.

MEZGER, K. & KROGSTAD, E. J. 1997. Interpretation of discordant U-Pb zircon ages: an evaluation. *Journal of Metamorphic Geology* **15**, 127–40.

MISHRA, S., DEOMURARI, M. P., WIEDENBECK, M., GOSWAMI, J. N., RAY, S. & SAHA, A. K. 1999. $^{207}Pb/^{206}Pb$ zircon ages and the evolution of the Singhbhum Craton, eastern India: an ion microprobe study. *Precambrian Research* **93**, 139–51.

MONDAL, M. E. A., GOSWAMI, J. N., DEOMURARI, M. P. & SHARMA, K. K. 2002. Ion microprobe $^{207}Pb/^{206}Pb$ ages zircons from Bundelkhand massif, north India: implications for crustal evolution of the Bundelkhand-Aravalli protocontinent. *Precambrian Research* **117**, 85–100.

MUKHOPADHYAY, J., BEUKES, N. J., ARMSTRONG, R. A., ZIMMERMANN, U., GHOSH, G. & MEDDA, R. A. 2008. Dating the oldest Greenstone in India, a 3.51-Ga precise U–Pb SHRIMP zircon age for Dacitic Lava of the Southern Iron Ore Group, Singhbhum Craton. *Journal of Geology* **116**, 449–61.

MYERS, J. S. 1988. Early Archaean Narryer Gneiss Complex, Yilgarn Craton, Western Australia. *Precambrian Research* **38**, 297–307.

NASDALA, L., HOFMEISTER, W., NORBERG, N., MATTINSON, J. M., CORFU, F., DÖRR, W., KAMO, S. L., KENNEDY, A. K., KRONZ, A., REINERS, P. W., FREI, D., KOŠLER, J., WAN, Y., GÖTZE, J., HÄGER, T., KRÖNER, A. & VALLEY, J. W. 2008. Zircon M257 – a homogeneous natural reference material for the ion microprobe U–Pb analysis of zircon. *Geostandards and Geoanalytical Research* **32**, 247–65.

NEBEL-JACOBSEN, Y., MUNKER, C., NEBEL, O., GERDES, A., MEZGER, K. & NELSON, D. 2010. Reworking of Earth's first crust: constraints from Hf isotopes in Archean zircons form Mt Narryer, Australia. *Precambrian Research* **182**, 175–86.

NUTMAN, A. P., BENNETT, V. C., FRIEND, C. R. L., HORIE, K. & HIKADA, H. 2007. 3,850 Ma tonalites in the Nuuk region, Greenland: geochemistry and their reworking within an Eoarchaean gneiss complex. *Contributions to Mineralogy and Petrology* **154**, 385–408.

NUTMAN, A. P., BENNETT, V. C., FRIEND, C. R. L. & MCGREGOR, V. R. 2000. The early Archaean Itsaq Gneiss Complex of southern West Greenland: the importance of field observations in interpreting age and isotopic constraints for early terrestrial evolution. *Geochimica et Cosmochimica Acta* **64**, 3035–60.

NUTMAN, A. P., CHADWICK, B., KRISHNA RAO, B. & VASUDEV, V. N. 1996. SHRIMP U–Pb zircon ages of acid volcanic rocks in the Chitradurga and Sandur Groups and granites adjacent to Sandur schist belt. *Journal of the Geological Society of India* **47**, 153–61.

NUTMAN, A. P., CHADWICK, B., RAMAKRISHNAN, M. & VISWANATHA, M. N. 1992. SHRIMP U–Pb ages of detrital zircon in Sargur supracrustal rocks in western Karnataka, Southern India. *Journal of the Geological Society of India* **39**, 367–74.

PATI, J. K., PATEL, S. C., PRUSETH, K. L., MALVIYA, V. P., ARIMA, M., RAJU, S., PATI, P. & PRAKASH, K. 2007. Geology and geochemistry of giant quartz veins from the Bundelkhand craton, Central India and their implications. *Journal of Earth System Science* **116**, 497–510.

PEUCAT, J.-J., MAHABALESHWAR, B. & JAYANANDA, M. 1993. Age of younger tonalitic magmatism and granulite metamorphism in the south Indian transition zone (Krishnagiri area): comparison with older peninsular gneisses from Hassan-Gorur area. *Journal of Metamorphic Geology* **11**, 879–88.

PEUCAT, J.-J., BOUHALLIER, H., FANNING, C. M. & JAYANANDA, M. 1995. Age of Holenarsipur greenstone belt, relationships with the surrounding gneisses (Karnataka, south India). *Journal of Geology* **103**, 701–10.

PRADHAN, V. R., MEERT, J. G., PANDIT, M. K., KAMENOV, G. & MONDAL, M. E. A. 2012. Paleomagnetic and geochronological studies of the mafic dyke swarms of Bundelkhand craton, central India: implications for the tectonic evolution and paleogeographic reconstructions. *Precambrian Research* **198–199**, 51–76.

RAJESH, H. M., MUKHOPADHYAY, J., BEUKES, N. J., GUTZMER, J., BELYANIN, G. A. & ARMSTRONG, R. A. 2009. Evidence of an early Archaean granite from Bastar Craton, India. *Journal of the Geological Society, London* **166**, 193–6.

RAMAKRISHNAN, M., VENKATADASU, S. P. & KRÖNER, A. 1994. Middle Archaean age of Sargur Group by single grain zircon dating and geochemical evidence for the clastic origin of metaquartzite from J.C. Pura Greenstone belt, Karnataka. *Journal of the Geological Society of India* **44**, 605–16.

RAM MOHAN, M., SINGH, S. P., SANTOSH, M., SIDDIQUI, M. A. & BALARAM, V. 2012. TTG suite from the Bundelkhand craton, central India: geochemistry, petrogenesis and implications for Archean crustal evolution. *Journal of Asian Earth Sciences* **58**, 38–50.

ROGERS, J. J. W. 1996. A history of continents in the past three billion years. *Journal of Geology* **104**, 91–107.

ROY, A. B., KRÖNER, A., RATHORE, S., LAUL, V. & PUROHIT, R. 2012. Tectono-metamorphic and geochronologic studies from Sandmata Complex, northwest Indian shield: implications on exhumation of Late-Palaeoproterozoic granulites in an Archaean–early Palaeoproterozoic granite-gneiss terrane. *Journal of the Geological Society of India* **79**, 323–34.

SAHA, A. K., BOSE, R., GHOSH, S. N. & ROY, A. 1977. Petrology and emplacement of Mayurbhanj Granite batholith, eastern India. *Evolution of orogenic belts of India (Part 2). Bulletin of the Geological Mineralogical Meteorological Society of India* **49**, 1–34.

SAHA, L., PANT, N. C., PATI, J. K., UPADHAYA, D., BERNDT, J., BHATTACHARYA, A. & SATYANARAYAN, M. 2011. Neoarchean high pressure margarite-phengitic muscovite- chlorite corona mantled corundum in quartz-free high-Mg, Al phlogopite-chlorite schists from the Bundelkhand craton, north-central India. *Contributions to Mineralogy and Petrology* **161**, 511–30.

SARKAR, G., CORFU, F., PAUL, D. K., MCNAUGHTON, N. J., GUPTA, S. N. & BISHUI, P. K. 1993. Early Archean crust in Bastar craton, central India – a geochemical and isotopic study. *Precambrian Research*, **62**, 127–37.

SARKAR, A., PAUL, D. K. & POTTS, P. J. 1996. Geochronology and geochemistry of Mid-Archean trondhjemitic

https://doi.org/10.1017/S0016756815000692 Published online by Cambridge University Press

gneisses from the Bundelkhand craton, central India. *Recent Researches in Geology* **16**, 76–92.

SENGUPTA, S., CORFU, F., MCNUTT, R. H. & PAUL, D. K. 1996. Mesoarchaean crustal history of the eastern Indian Craton – Sm–Nd and U–Pb isotopic evidence. *Precambrian Research* **77**, 17–22.

SHARMA, K. K. & RAHMAN, A. 2000. The Early Archaean–Paleoproterozoic crustal growth of the Bundelkhand craton, northern Indian shield. In *Crustal Evolution and Metallogeny in the Northwestern Indian Shield* (ed. M. Deb), pp. 51–72. New Delhi: Narosa Publishing House.

SINGH, V. K. & SLABUNOV, A. 2014. The Central Bundelkhand Archean greenstone complex, Bundelkhand craton, central India: geology, composition, and geochronology of supracrustal rocks. *International Geology Review* **57**, 1349–64.

SLÁMA, J., KOŠLER, J., CONDON, D. J., CROWLEY, J. L., GERDES, A., HANCHAR, J. M., HORSTWOOD, M. S. A., MORRIS, G. A., NASDALA, L., NORBERG, N., SCHALTEGGER, U., SCHOENE, B., TUBRETT, M. N. & WHITEHOUSE, M. J. 2008. Plešovice zircon—a new natural reference material for U–Pb and Hf isotopic microanalysis. *Chemical Geology* **249**, 1–35.

STACEY, J. S. & KRAMERS, J. D. 1975. Approximation of terrestrial Pb isotope evolution by a two-stage model. *Earth and Planetary Science Letters* **26**, 207–21.

VAN KRANENDONK, M. J., SMITHIES, R. H. & BENNETT, V. C. (eds) 2007. *Earth's Oldest Rocks*. Developments in Precambrian Geology 15. Amsterdam: Elsevier, 856 pp.

WIEDENBECK, M. & GOSWAMI, J. N. 1994. An ion-probe single zircon $^{207}Pb/^{206}Pb$ age from the Mewar Gneiss at Jhamarkotra, Rajasthan. *Geochimica et Cosmochimica Acta* **58**, 2135–41.

WILDE, S. A., VALLEY, J. W., PECK, W. H. & GRAHAM, C. M. 2001. Evidence from detrital zircons for the existence of continental crust and oceans on the Earth 4.4 Gyr ago. *Nature* **409**, 175–8.

ZEH, A., GERDES, A. & MILLONIG, L. 2011. Hafnium isotope record of the Ancient Gneiss Complex, Swaziland, southern Africa: evidence for Archaean crust–mantle formation and crust reworking between 3.66 and 2.73 Ga. *Journal of the Geological Society, London* **168**, 953–63.

https://doi.org/10.1017/S0016756815000692 Published online by Cambridge University Press